Ab Initio Direct Dynamics Studies on the Reactions of H Atoms with CCl_4 and $CHCl_3$

Li Sheng, Ze-Sheng Li,* Jing-Yao Liu, Jing-Fa Xiao, and Chia-Chung Sun

Institute of Theoretical Chemistry, State Key Laboratory of Theoretical and Computational Chemistry, Jilin University, Changchun 130023, P. R. China

Received: September 19, 2002; In Final Form: October 25, 2002

By means of ab initio direct dynamics method, the reactions H + CCl_4 → CCl_3 + HCl (1) and H + $CHCl_3$ → products (2) have been investigated theoretically to reveal their dynamical properties. The minimum energy paths (MEPs) of both reactions are calculated at the BH&H-LYP/6-311G(d,p) level, and the energies along the MEPs are further refined at the PMP4/6-311+G(3df,2p) (single-point) level. For reaction 2, both reaction channels, H-abstraction and Cl-abstraction, have been identified. Thus, the rate constants for each reaction channel as well as reaction 1 are calculated by the canonical variational transition state theory incorporating the small-curvature tunneling correction in the temperature range 200−5000 K. For reaction 1, the theoretical rate constants are in good agreement with the experimental values over the measured temperature range. For reaction 2, the total rate constants, which are calculated from the sum of the individual rate constants, are in excellent agreement with the experimental ones, and the temperature dependence of the branching ratios indicate that, at low-temperature range (T < 667 K), H-abstraction is the major reaction channels, whereas Cl-abstraction channels will significantly contribute to the whole reaction rate as the temperature increases.

Introduction

The importance of chlorinated hydrocarbons (CHCs) in atmospheric chemistry is well established.[1,2] Chloromethanes are known to be important atmospheric species and should be responsible for the depletion of the ozone layer in the stratosphere and for the greenhouse effects. To incinerate the industrial wastes CHCs in a more efficient and less hazardous way, it is necessary to further investigate all aspects of this kind of combustion process. It is especially important to understand the incineration mechanism, specific pathways, and rate constants for important elementary reactions. The current studied reactions play an important role in the incineration of chlorinated hydrocarbons. For example, in CHC/O_2 and CHC/hydrocarbon/O_2 flames, reactions of H and Cl with CHCs together with unimolecular decomposition are the major channels of consumption of CHCs.[3−15] In fuel-rich flames, the reactions of H atom with CHCs compete directly with the main chain-branching reaction, H + O_2 → OH + O.[3,16−18]

Although the importance of the H + CHCs reactions has been shown, little is known about the rate of even the chlorinated methanes, the simplest CHC reactions. In the most recent work,[19] the direct measurement of the overall rates for following reactions

$$H + CCl_4 \rightarrow HCl + CCl_3 \ (297-904\ K) \qquad (1)$$

$$H + CHCl_3 \rightarrow \text{products}\ (455-854\ K) \qquad (2)$$

was reported by Bryukov and co-workers. (Numbers in parentheses denote the experimental studied temperature ranges.) For reaction 2, it can proceed through the abstraction of both chlorine and hydrogen atoms, i.e.

$$H + CHCl_3 \rightarrow HCl + CHCl_2 \qquad (2a)$$

$$H + CHCl_3 \rightarrow H_2 + CCl_3 \qquad (2b)$$

while up to now, no experimental information is available on the branching ratio $k_{2a}/(k_{2a} + k_{2b})$; therefore, theoretical investigations are very desirable to give an understanding of the multiple channel reaction mechanisms of the reaction H + $CHCl_3$. Bryukov et al. have studied the branching ratio of reaction 2 within the framework of conventional transition state theory (TST) with an application of the Marcus equation, and their calculated results have indicated that reaction 2b is a minor reaction channel, where the contribution to the whole reaction is 5∼10% in the experimental temperature range. However, under their investigation, one-dimensional Eckart tunneling correction associated with the TST framework may not be sufficient, because the tunneling contributions to the rate of hydrogen abstraction reactions are significant.[20,21] In this paper, the main aim is to perform a direct ab initio dynamics study at relatively higher level on the total rate constants of the title reactions and the branching ratio of reaction 2 over the temperature range 200−5000 K in order to obtain more reliable results.

Calculation Methods

It has been previously shown[22−25] that the combination of Becke's half-and-half (BH&H)[26] with Lee−Yang−Parr (LYP)[27] nonlocal correlation functionals can be used cost-effectively to calculate the geometries and frequencies particularly for open-shell systems. In the present work, the equilibrium geometries and frequencies of the stationary points (reactants, products, and

* To whom correspondence should be addressed.

10.1021/jp022109u CCC: $22.00
Published on Web 11/22/2002

TABLE 1: Calculated and Experimental Frequencies (cm^{-1}) of Stationary Points for the Three Reactions

species	BH&H-LYP/6-311G(d,p)	expt
$CHCl_3$	277, 277, 384, 695, 802, 802, 1309, 1309, 3288	261, 261, 363, 680, 774, 774, 1220, 1220, 3034[a]
$CHCl_2$	317, 484, 779, 920, 1304, 3325	902, 1226[b]
$CCl_2H\cdots Cl'\cdots H$(TS)	1021*i*, 202, 224, 262, 268, 364 654, 765, 834, 1192, 1311, 3293	
$CCl_3\cdots H'\cdots H$ (TS)	1734*i*, 276, 276, 354, 354, 394, 622, 842, 842, 1283, 1283, 1497	
CCl_3	289, 289, 331, 509, 933, 933	266, 266, −, 487, 898, 898[b]
CCl_4	233, 332, 477, 814, 814	217, 314, 459, 776, 776[c]
$CCl_3\cdots Cl'\cdots H$ (TS)	965*i*, 189, 189, 230, 230, 319, 319, 320, 469, 747 838, 838	
HCl	3046	2991[a]
H_2	4518	4403[d]

[a] Experimental values from ref 36. [b] Experimental values from ref 37. [c] Experimental values from ref 38. [d] Experimental values from ref 39.

transition states) are calculated by using the BH&H-LYP method with the 6-311G(d,p) basis set by using Gaussian 98 program package.[28] At the same level, the minimum energy path (MEP) is obtained by intrinsic reaction coordinate theory (IRC) with a gradient step size of 0.05 $(amu)^{1/2}$ bohr. Furthermore, with selected points along the MEP, the force constant matrixes as well as the harmonic vibrational frequencies are obtained. To obtain more accurate energy along the MEP, the spin-projected fourth-order Møller−Plesset perturbation theory (PMP4) calculations are performed using 6-311+G(3df,2p) basis set at the BH&H-LYP MEP geometries, for simplicity, hereinafter it is denoted by PMP4//BH&H-LYP.

Canonical variational transition state theory (CVT) is based on the idea of varying the dividing surface along a reference path to minimize the rate constants; thus, this method is more accurate than the TST one. In this paper, the POLYRATE version 8.4.1 program[29] is performed to obtain the theoretical rate constants in the temperature range 200−5000 K using the CVT plus a small-curvature tunneling (SCT) correction method proposed by Truhlar and co-workers.[30,31] The Euler single-step integrator with a step size of 0.0001 $(amu)^{1/2}$bohr is used to follow the MEP, and the generalized normal-mode analysis is performed in every 0.01 $(amu)^{1/2}$bohr.

Results and Discussions

1. Stationary Points. The optimized geometric parameters of the reactants ($CHCl_3$ and CCl_4) and products ($CHCl_2$, CCl_3, and HCl) at the BH&H-LYP/6−311G(d,p) level of theory are presented in Figure 1a along with the available experimental data.[32−35] From Figure 1a, we can see that the largest deviation between the theoretical bond lengths and the experimental values is 0.028 Å (r(C−Cl) for CCl_3) and the largest deviation of the bond angles is 2.8° for ∠ClCCl in CCl_3. It is obvious that the theoretical geometric parameters are in good agreement with the experimental data.[32−35]

Geometric parameters of the transition state structures for the three reactions are depicted in Figure 1b. From Figure 1b, we can see that the transition states TS1 for reaction 1 and TS2b for reaction 2b have the same symmetry, i.e., C_{3v} symmetry. For reaction 2a, the transition state (TS2a) has C_s symmetry. In the transition state structures, the distance of the bonds C−Cl′ and C−H′, which will be broken, increase by 7.2%, 8.2%, and 20% with respect to the equilibrium bond distances of CCl_4 and $CHCl_3$ in the reactions 1, 2a, and 2b, respectively. The distances of H−Cl′ and H−H′, which will form molecules, are 1.37, 1.42, and 1.3 times, respectively, as large as the equilibrium bond distances in HCl and H_2 molecules. Therefore, the three transition states are all reactant-like, and the reactions will proceed via early transition states. It is obvious that the TS2a is a more reactant-like TS, so the chlorine abstraction reaction 2a will proceed via an "earlier" transition state compared with hydrogen abstraction reaction 2b.

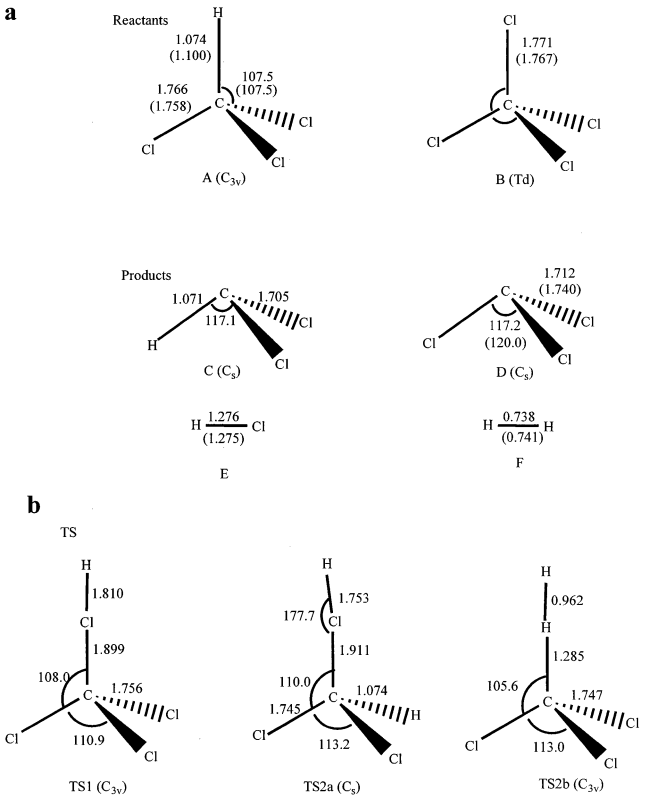

Figure 1. a. Optimized geometries of reactants and products at the BH&H-LYP/6-311G(d,p) level of theory. The numbers in parentheses are the experimental values[32−35] [ref 32 for $CHCl_3$ (A) and HCl (E), ref 33 for CCl_4 (B), ref 34 for CCl_3 (D), ref 35 for H_2 (F)]. Bond lengths are in angstroms, and angles are in degrees. b. Optimized geometries of the three transition states at the BH&H-LYP/6-311G(d,p) level of theory. Bond lengths are in angstroms, and angles are in degrees.

Table 1 gives the harmonic vibrational frequencies of the reactants, products, and transition states at the BH&H-LYP/6-311G(d,p) level as well as the corresponding experimental results.[36−39] For the species of reactants and products, the calculated frequencies are in good agreement with the experimental values with the largest deviation of 8%. For each transition state, the character of the stationary point is confirmed by normal-mode analysis, which yields one and only one imaginary frequency whose eigenvector corresponds to the direction of the reaction.

The reaction enthalpies ($\Delta H°_{298}$) and classical barrier heights (ΔE^f) calculated at the PMP4//BH&H-LYP level of theory with ZPE correction are listed in Table 2. For the reactions 2a and 2b, the calculated reaction enthalpies at temperature 298 K are −27.4 and −10.4 kcal/mol, respectively, which are in good agreement with the corresponding experimental values of −28.4 and −10.6 kcal/mol derived from the experimental standard heats of formation ($CHCl_3$, −25.6 kcal/mol;[40] H, 52.1 kcal/

TABLE 2: Reaction Enthalpies (ΔH^0_{298}) and Forward Potential Barriers (ΔE^f) (kcal/mol) with ZPE Correction for the Three Reactions at PMP4//BH&H-LYP Level of Theory

	$CCl_4 + H \rightarrow CCl_3 + HCl$	$CHCl_3 + H \rightarrow CHCl_2 + HCl$	$CHCl_3 + H \rightarrow CCl_3 + H_2$
ΔE^f	6.5	8.0	6.8
ΔH°_{298}	−28.9	−27.4	−10.4
expt[a]	−34.3	−28.4	−10.6

[a] Experimental values derived from heats of formation (in kcal/mol): $CHCl_3$, −25.6;[40] H, 52.1;[41] $CHCl_2$, 21.3;[42] HCl, −22.1;[41] CCl_3, 17.0;[43] H_2, 0.0; CCl_4, −22.9.[40]

mol;[41] $CHCl_2$, 21.3 kcal/mol;[42] HCl, −22.1 kcal/mol;[41] CCl_3, 17.0 kcal/mol;[43] H_2, 0.0 kcal/mol). The barrier height for reaction 2a is 8.0 kcal/mol and for reaction 2b is 6.8 kcal/mol obtained at the PMP4//BH&H-LYP level of theory; that is, the H-abstraction reaction 2b has a lower barrier height compared to Cl-abstraction reaction 2a, and as a result, H-abstraction reaction 2b will be preferred at lower temperatures. This view is further testified in the following study of the rate constants. For the H + CCl_4 reaction, the calculated reaction enthalpy value of −28.9 kcal/mol is in reasonable agreement with the estimated value of −34.3 kcal/mol (CCl_4, −22.9 kcal/mol;[40]), and the barrier height is 6.5 kcal/mol at PMP4//BH&H-LYP level of theory.

2. Minimum Energy Path. The changes of bond lengths along the IRC for H reacted with CCl_4 are plotted in Figure 2a. It is easily seen that with the proceeding of this reaction, the active C−Cl′ (breaking) bond length changes very smoothly up to about $s = -1.0$ (amu)$^{1/2}$ bohr, after that, the C−Cl′ bond length increases slightly. Although the H−Cl′ (forming) bond length decreases linearly along the reaction coordinate from $s = -2.0$ to 1.0 (amu)$^{1/2}$bohr, and after $s = 1.0$ (amu)$^{1/2}$bohr, the change of the H−Cl′ both bond length becomes slow. However, the lengths of the other bond show nearly no change during the entire reaction processes. For the remaining tow reactions, i.e., H + $CHCl_3 \rightarrow$ HCl + $CHCl_2$ and H + $CHCl_3 \rightarrow$ H_2 + CCl_3, the bond length changes along the IRC are similar to reaction H + CCl_4.

Figure 3a−c depicts the classical potential energy, V_{MEP}, the ground-state vibrational adiabatic potential energy, V_a^G, and the zero-point energy ZPE for the three reactions as functions of the reaction coordinate s ((amu)$^{1/2}$ bohr) at the PMP4//BH&H-LYP level of theory. For the three reactions, the maximum positions of the $V_{MEP}(s)$ and $V_a^G(s)$ energy curve are the same, and the zero-point energy curves are practically constants as s varies with only a gentle fall near the saddle point ($s = 0$). To analyze this behavior in more detail, we show the variations of generalized normal mode vibrational frequencies along the MEP in Figure 4a−c. In the negative limit of s, the frequencies are associated with the reactants H + CCl_4 and H + $CHCl_3$, respectively. In the positive limit of s, the frequencies are associated with the products HCl + CCl_3, HCl + $CHCl_2$, and H_2 + CCl_3, respectively. Now let us turn our attention to the frequencies in the vicinity of the transition state. The harmonic vibrational frequencies of the C−Cl′ and C−H′ stretches shown by the mode 11 in Figure 4a−c, corresponding to the generalized normal mode that breaks during the reactions, rapidly drop near the saddle point. These drops should cause considerable falls in the ZPE near the saddle point. On the other hand, the two lowest harmonic frequencies corresponding to free rotations and translations of the reactants evolve to vibrations at about $s = -0.3$ (amu)$^{1/2}$ bohr, and they present a maximum near the saddle point. The behaviors of these two lowest frequencies counteract the decreases in the ZPE caused by the C−Cl′ and C−H′ stretches, respectively. As a result, the ZPE has a little change

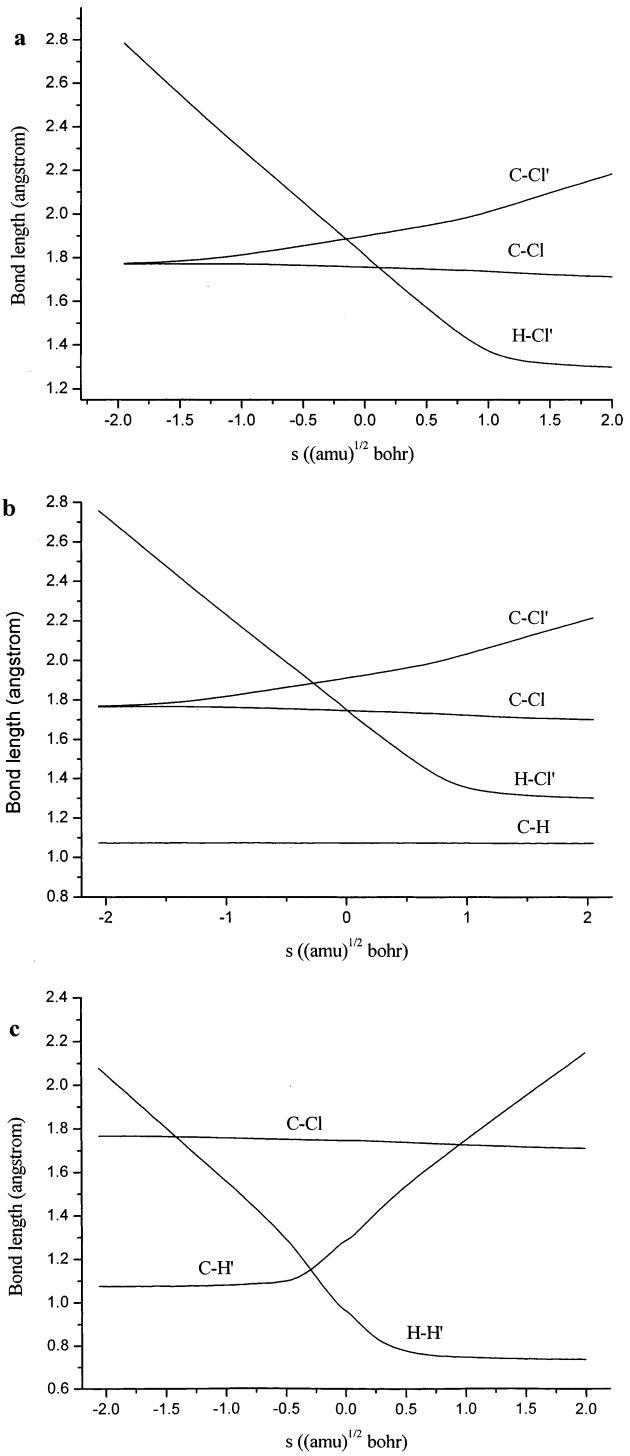

Figure 2. a. Changes of the bond lengths along the BH&H-LYP/6-311G(d,p) minimum energy path for the H + $CCl_4 \rightarrow$ HCl + CCl_3 reaction plotted vs the reaction coordinate s in the mass weighted coordinates. b. Same types of curves as those in a for the H + $CHCl_3 \rightarrow$ HCl + $CHCl_2$ reaction. c. Same types of curves as those in a for the H + $CHCl_3 \rightarrow$ H_2 + CCl_3 reaction.

with s. For the classical potential energy V_{MEP} and the ground-state vibrational adiabatic potential energy V_a^G curves, the shapes are similar. This analysis indicates that, for the three reactions, the variational effect on the calculation of rate constant will be small.

3. Rate Constants. The canonical variational transition state theory (CVT) rate constants with a small-curvature tunneling correction (SCT) for the three reactions are calculated in a wide

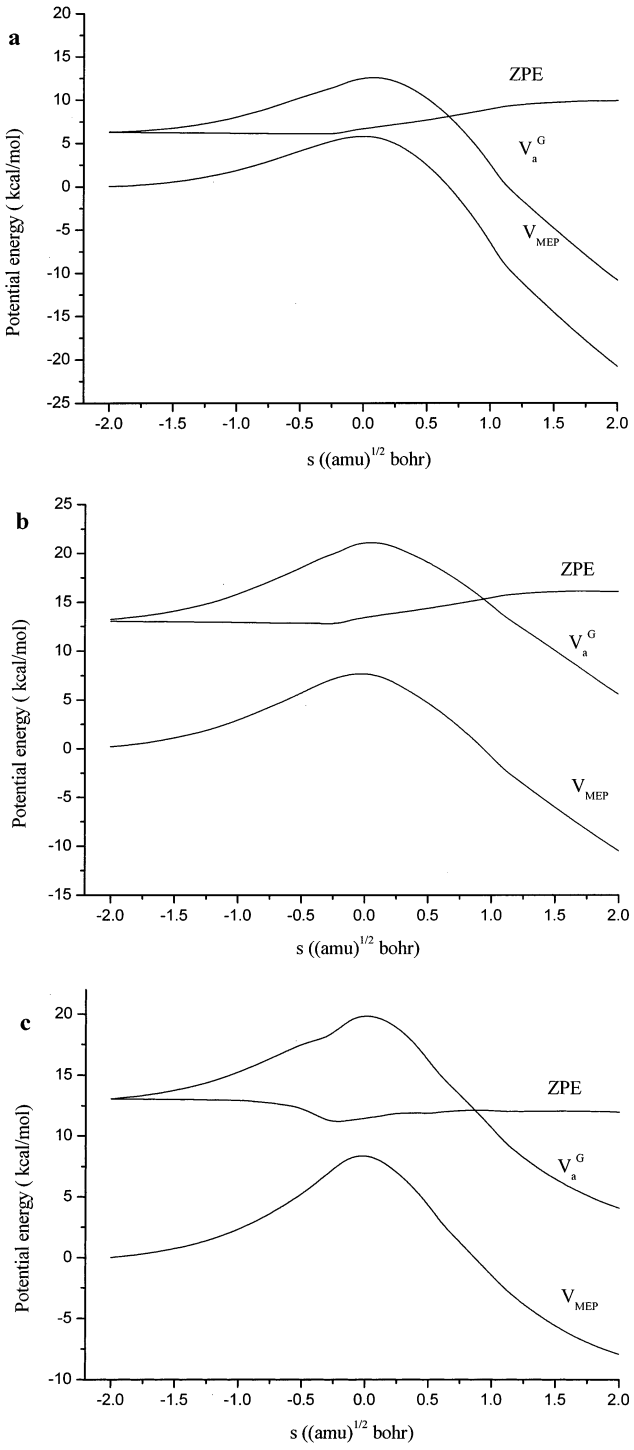

Figure 3. a. Classical potential energy (V_{MEP}), zero-point energies (ZPE), and vibrational adiabatic potential energy (V_a^G) as a function of the reaction coordinate, *s*, at the PMP4//BH&H-LYP level for the H + CCl_4 → HCl + CCl_3 reaction. b. Same types of curves as those in a for the H + $CHCl_3$ → HCl + $CHCl_2$ reaction. c. Same types of curves as those in a for the H + $CHCl_3$ → H_2 + CCl_3 reaction.

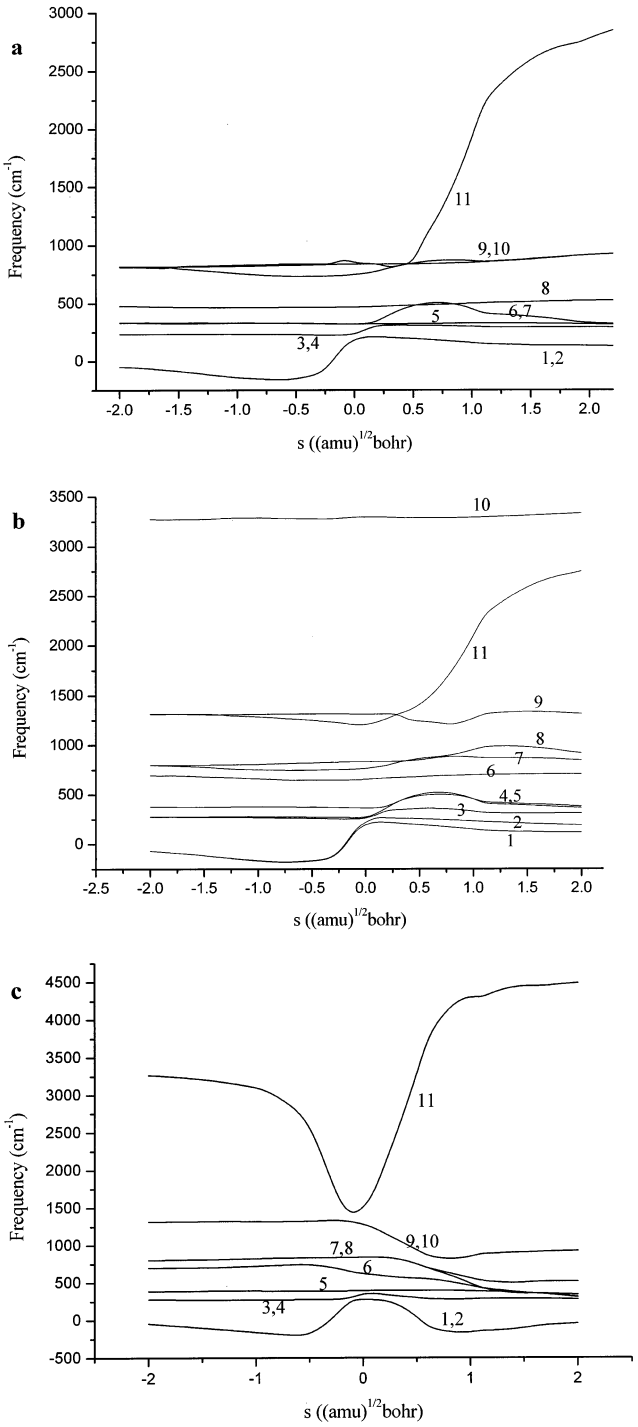

Figure 4. a. Change of the generalized normal-mode vibrational frequencies for the H + CCl_4 → HCl + CCl_3 reaction as functions of the reaction coordinate, *s*, at the BH&H-LYP/6-311G(d,p) level. b. Same types of plots as those in a for the H + $CHCl_3$ → HCl + $CHCl_2$ reaction. c. Same types of plots as those in a for the H + $CHCl_3$ → H_2 + CCl_3 reaction.

temperature range from 200 to 5000 K at the PMP4//BH&H-LYP level of theory. Figure 5 displays the calculated rate constants and the available experimental values[19] for the H + CCl_4 reaction. It can be seen that the TST and CVT rate constants are nearly the same over the whole temperature range, whereas the CVT/SCT rate constants are significantly larger than the CVT rate constants in the lower temperature range and they are asymptotic to the CVT one at the higher temperatures. This means that for this reaction the variational effect is small over the whole temperature range and the small-curvature tunneling correction (SCT) plays an important part in the lower temperature range. In comparison of our theoretical results with the experimental ones, the CVT/SCT rate constants are in good agreement with the available experimental values in the experimental temperature range. The theoretical rate constants are factors of 2.8, 2.7, 2.5, 2.3, 1.9, 1.8, and 1.7 lower than the experimental values at 297, 325, 381, 456, 690, 854, and 904 K, respectively. Our calculated value of activation energy is 6.3 kcal mol^{-1} and much close to the experimental value of

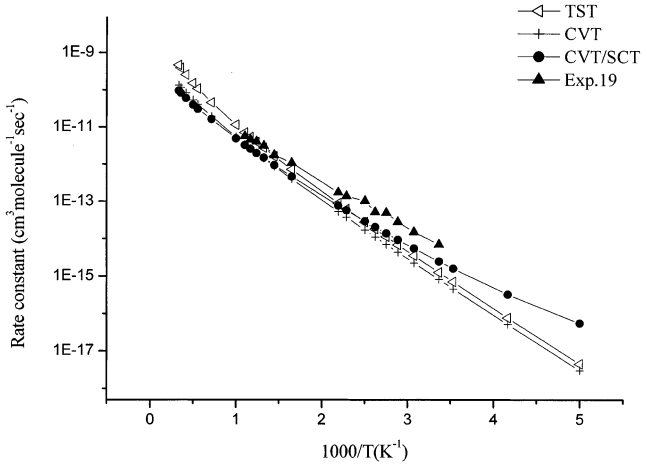

Figure 5. Computed TST, CVT, and CVT/SCT rate constants as a function of 10^3/T and available experimental values for H + CCl_4 → HCl + CCl_3 reaction.

5.8 kcal mol^{-1}. Because the temperatures used in the experiments[19] to determine the rates of the reaction are still far from covering the whole temperature range of practical interest, which extends to the temperatures of combustion, i.e., up to 2000−2500 K, and our calculated results agree well with experimental ones both in rate constants and activation energy. Our results may provide useful information for future experimental measurements. The three-parameter fits for the CVT/SCT rate constants for the reaction from 200 to 5000 K give the expression as follows: $k = 2.31 \times 10^{-15}\, T^{1.43} \exp(-2374.5/T)$ cm^3 molecules^{-1} s^{-1}.

For reactions 2a and 2b, the CVT/SCT rate constants of k_{2a}, k_{2b}, and total rate constants, k_2 with $k_2 = k_{2a} + k_{2b}$, as well as the experimental ones[19] are plotted against 1000/T in Figure 6a, and the temperature dependence of the k_{2a}/k_2 and k_{2b}/k_2 branching ratios is exhibited in Figure 6b. From Figure 6a, we can see that, at temperature lower than 400 K, k_{2b} is about 1 order of magnitude larger than k_{2a}, and the total rate constant is nearly equal to the rate constant of reaction 2b. Thus, the H abstraction is likely to dominate the reaction at lower temperatures. However, as shown in Figure 6b, the contribution of k_{2b} to the total rate constant decreases with the increase of the temperature, for example, the k_{2b}/k_2 ratios are 99% at 200 K, 94% at 297 K, 86% at 363 K, 65% at 503 K, 50% at 667 K, 40% at 904 K, and 35% at 1500 K. It is also shown that, at a temperature higher than 667 K, the rate constants of Cl abstraction, k_{2a}, become faster than k_{2b}. Consequently, both reaction channels will contribute to the whole reaction rate as the temperature increases. This result is significantly different from that obtained by Bryukov[19] and co-workers based on TST calculation with one-dimensional tunneling correction for the H-abstraction reactions. Under their investigation, the H-abstraction reaction contribution to the whole reaction is 5∼10% in the experimental temperature range 455−854 K. The possible reason may be that Bryukov et al. just performed TST calculations followed by a crude estimate of a one-dimensional (1D) approach of the tunneling factor in the reaction instead of calculating the analytical potential energy surface (PES), and the shape of PES is very important for determination of the reaction rate constants. Our investigation shows that the tunneling contributions in hydrogen abstraction reactions are also significant as pointed by Truong and co-workers[20,21] and it can be seen from Figure 7a,b, where the TST, CVT, and CVT/SCT rate constants for reaction 2a and 2b are plotted. For the H + $CHCl_3$ → H_2 + CCl_3 reaction, the k(CVT/SCT)/k(SCT) ratios are 405, 48, 34, 11, 4.1, and 2.0 at 200, 283, 298, 363, 483, and 690 K, respectively, whereas for the H + $CHCl_3$ → HCl + $CHCl_2$ reaction, the ratios are 28, 4.0, 3.4, 2.1, 1.4, and 1.1 at the corresponding temperature points. Thus, the small-curvature tunneling (SCT) correction plays an important role in the lower temperature region for both reactions. In comparison with Cl-abstraction reaction, the tunneling correction is more important for the rate constant calculations of H-abstraction reaction. This may imply that the hydrogen abstraction reaction is the major destruction pathways in the H + $CHCl_3$ reaction at a temperature lower than 667 K. In addition, from Figure 7a,b, we can see the TST and CVT rate constants are nearly the same in the whole temperature range, which enables us to conclude that the variational effect for the two reactions is very small.

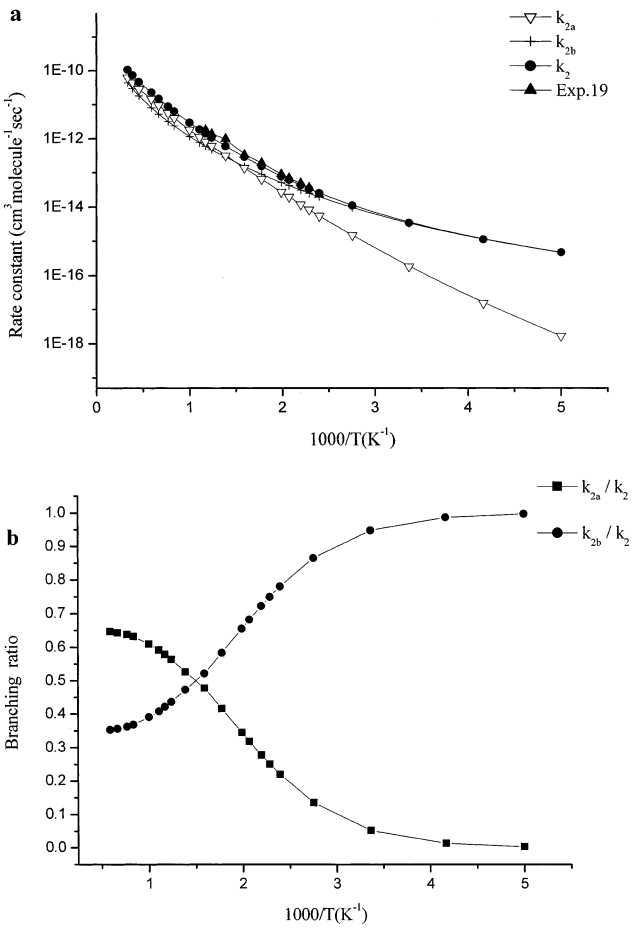

Figure 6. a. Calculated individual rate constants, k_{2a} for the H + $CHCl_3$ → HCl + $CHCl_2$ reaction, k_{2b} for the H + $CHCl_3$ → H_2 + CCl_3 reaction, and total rate constants k_2 along with experimental values as a function of $10^3/T$. b. Calculated branching ratio for the H + $CHCl_3$ reaction as a function of 10^3/T.

From Figure 6a, we can see that the total rate constants (k_2) of the reaction H + $CHCl_3$ are in excellent agreement with the experimental values[19] in the measured temperature range 455−854 K. The k(expt)/k(CVT/SCT) ratios are 1.0, 1.1, 1.2, 1.3, and 1.3 at the 455, 503, 629, 807, and 854 K, respectively. Therefore, it is reasonable to think that the theoretical results obtained at the PMP4//BH&H-LYP level of theory are reliable over the entire temperature region. Finally, for convenience of future experimental measurements, we give three-parameter rate constant expressions by fitting the theoretical results for the H + $CHCl_3$ reaction over the whole temperature range 200−5000 K, and the expressions are (in units of cm^3 molecules^{-1} s^{-1}) as

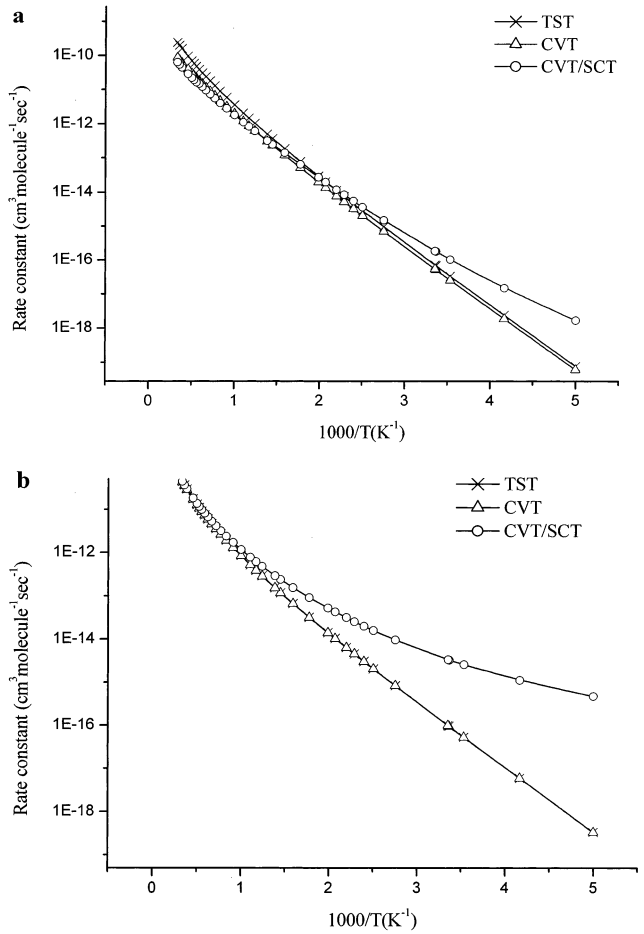

Figure 7. a. Computed TST, CVT, and CVT/SCT rate constants as a function of $10^3/T$ for the $H + CHCl_3 \rightarrow HCl + CHCl_2$ reaction. b. Same types of plots as those in a for the $H + CHCl_3 \rightarrow H_2 + CCl_3$ reaction.

follows: $k_{2a} = 5.1 \times 10^{-16}\, T^{1.59} \exp(-2948.6/T)$, $k_{2b} = 7.15 \times 10^{-20}\, T^{2.85} \exp(-912.9/T)$, and $k_2 = 3.87 \times 10^{-20}\, T^{2.77} \exp(-1242.1/T)$.

Conclusions

In this paper, the reactions $H + CCl_4 \rightarrow HCl + CCl_3$ (1), $H + CHCl_3 \rightarrow HCl + CHCl_2$ (2a), and $H + CHCl_3 \rightarrow H_2 + CCl_3$ (2b) have been studied by ab initio direct dynamics method. For the three reactions, the calculated potential barriers at the PMP4//BH&H-LYP level are 6.5, 8.0, and 6.8 kcal mol^{-1}, respectively, and the corresponding reaction enthalpy are -34.3, -28.4, and -10.6 kcal mol^{-1}. The theoretical rate constants in the temperature range 200−5000 K are calculated by the canonical variational transition state theory (CVT) with the small-curvature tunneling correction (SCT). The calculated total rate constants of these reactions are in good agreement with the corresponding experimental values over the measured temperature range. For the $H + CHCl_3$ reaction, the H-abstraction reaction will be preferred in the lower temperature range ($T < 667$ K), whereas as the temperature increases, the contribution of the Cl-abstraction reaction channels should be taken into account, and the reaction will proceed in favor of Cl abstraction at higher temperature range. Moreover, the calculated results show that, for the three reactions, the variational effect on the calculation of rate constants is small over the whole temperature range, and the tunneling correction plays an important role in the lower temperature range.

Acknowledgment. The authors thank Professor Donald G. Truhlar for providing the POLYRATE 8.4.1 program. This work is supported by the National Science Foundation of China (29892168, 20073014), Doctor Foundation by the Ministry of Education, Foundation for University Key Teacher by the Ministry of Education, and Key subject of Science and Technology by the Ministry of Education of China.

References and Notes

(1) (a) Tuck, R.; Plumb, A.; Condon, E. *Geophys. Res. Lett.* **1990**, *17*, 313. (b) Rosswall, T. *Environ. Sci. Technol.* **1991**, *25*, 567.

(2) (a) Atkinson, R. *Chem. Rev.* **1986**, *86*, 69. (b) Atkinson, R. *J. Phys. Chem. Ref. Data*. **1994**, Monograph 2.

(3) Karra, S. B.; Gutman, D.; Senkan, S. M. *Combust. Sci. Technol.* **1988**, *60*, 45.

(4) Chang, W. D.; Senkan, S. M. *Environ. Sci. Technol.* **1989**, *23*, 442.

(5) Lee, K. Y.; Yang, M. H.; Puri, I. K. *Combust. Flame* **1993**, *92*, 419.

(6) Wang, H.; Hahn, T. O.; Sung, C. J.; Law, C. K. *Combust. Flame* **1996**, *105*, 291.

(7) Chang, W. D.; Karra, S. B.; Senkan, S. M. *Combust. Sci. Technol.* **1986**, *49*, 107.

(8) Xieqi, M.; Cicek, B.; Senkan, S. M. *Combust. Flame* **1993**, *94*, 131.

(9) Cicek, B.; Senkan, S. M. *Combust. Sci. Technol.* **1993**, *91*, 53.

(10) Cui, J. P.; He, Y. Z.; Tsang, W. *J. Phys. Chem.* **1989**, *93*, 724.

(11) Lee, K. Y.; Puri, I. K. *Combust. Flame* **1993**, *92*, 440.

(12) Lee, K. Y.; Puri, I. K. *Combust. Flame* **1993**, *94*, 191.

(13) Taylor, P. H.; Tirey, D. A.; Dellinger, B. *Combust. Flame* **1996**, *104*, 260.

(14) Taylor, P. H.; Tirey, D. A.; Dellinger, B. *Combust. Flame* **1996**, *106*, 1.

(15) Ho, W. P.; Yu, Q.-R.; Bozzelli, J. W. *Combust. Sci. Technol.* **1992**, *85*, 23.

(16) Karra, S. B.; Senkan, S. M. *Combust. Sci. Technol.* **1987**, *54*, 333.

(17) Tsang, W. *Combust. Sci. Technol.* **1990**, *74*, 99.

(18) Combourieu, J.; Le Bras, G.; Paty, C. *Symp. Int. Combust. Proc.* **1973**, *14*, 485.

(19) Bryukov, M. G.; Slagle, I. R.; Knyazev, V. D. *J. Phys. Chem. A* **2001**, *105*, 3107.

(20) Maity, D. K.; Duncan, W. T.; Truong, T. N. *J. Phys. Chem. A* **1999**, *103*, 2152.

(21) Truong, T. N.; Duncan, W. T.; Tirtowidjojo, M. *Phys. Chem. Chem. Phys.* **1999**, *1*, 1061.

(22) Duncan, W. T.; Truong, T. N. *J. Chem. Phys.* **1995**, *103*, 9642.

(23) Truong, T. N.; Duncan, W. T.; Bell, R. L. *Chemical Applications of Density-Functional Theory*; Americal Chemical Society: Washington, DC, 1996; p 85.

(24) Truong, T. N. *J. Chem. Phys.* **1994**, *100*, 8014.

(25) Maity, D. K.; Duncan, W. T.; Truong, T. N. *J. Phys. Chem. A* **1999**, *103*, 2152.

(26) Becke, A. D. *J. Chem. Phys.* **1993**, *98*, 1372.

(27) Lee, C.; Yang, W.; Parr, R. G. *Phys. Rev. B* **1988**, *37*, 785.

(28) Frisch, M. J.; Trucks, G. W.; Schlegel, H. B.; Scuseria, G. E.; Robb, M. A.; Cheeseman, J. R.; Zakrzewski, V. G.; Montgomery, J. A., Jr.; Stratmann, R. E.; Burant, J. C.; Dapprich, S.; Millam, J. M.; Daniels, A. D.; Kudin, K. N.; Strain, M. C.; Farkas, O.; Tomasi, J.; Barone, V.; Cossi, M.; Cammi, R.; Mennucci, B.; Pomelli, C.; Adamo, C.; Clifford, S.; Ochterski, J.; Petersson, G. A.; Ayala, P. Y.; Cui, Q.; Morokuma, K.; Malick, D. K.; Rabuck, A. D.; Raghavachari, K.; Foresman, J. B.; Cioslowski, J.; Ortiz, J. V.; Stefanov, B. B.; Liu, G.; Liashenko, A.; Piskorz, P.; Komaromi, I.; Gomperts, R.; Martin, R. L.; Fox, D. J.; Keith, T.; Al-Laham, M. A.; Peng, C. Y.; Nanayakkara, A.; Gonzalez, C.; Challacombe, M.; Gill, P. M. W.; Johnson, B. G.; Chen, W.; Wong, M. W.; Andres, J. L.; Head-Gordon, M.; Replogle, E. S.; Pople, J. A. *Gaussian 98*, revision A.7; Gaussian, Inc.: Pittsburgh, PA, 1998.

(29) Chang, Y.-Y.; Corchado, J. C.; Fast, P. L.; Villa, J.; Hu, W.-P.; Liu, Y.-P.; Lynch, G. C.; Jackels, C. F.; Nguyen, K. A.; Gu, M. Z.; Rossi, I.; Coitino, E. L.; Clayton, S.; Melissas, V. S.; Lynch, B. J.; Steckler, R.; Garrett, B. C.; Isaacson, A. D.; Truhlar, D. G. *POLYRATE*, version 8.4.1; University of Minnesota: Minneapolis, MN, 2000.

(30) Truhlar, D. G.; Isaacson, A. D.; Garrett, B. C. Generalized Transition State Theory. In *The Theory of Chemical Reaction Dynamics*; Baer, M., Ed.; CRC Press: Boca Raton, FL, 1985; Vol. 4, p 65.

(31) Steckler, R.; Hu, W.-P.; Liu, Y.-P.; Lynch, G. C.; Garrett, B. C.; Isaacson, A. D.; Melissas, V. S.; Lu, D.-P.; Troung, T. N.; Rai, S. N.; Hancock, G. C.; Lauderdale, J. G.; Joseph, T.; Truhlar, D. G. *Comput. Phys. Commun.* **1995**, *88*, 341.

(32) Huber, K. P.; Herzberg, G. *Molecular Spectra and Molecular Structure*. *IV*. *Constants of Diatomic Molecules*; Van Nostrand Reinhold Co.: New York, 1979.

(33) Morino, Y.; Nakamura, Y.; Iijima, T. *J. Chem. Phys.* **1960**, *32*, 643.

(34) Milligan, D. E.; Jacox, M. E.; McAuley, J. H.; Smith, C. E. *J. Mol. Spectrosc*. **1973**, *45*, 377.

(35) Lide, D. R. In *CRC Handbook of Chemistry and Physics*, 73rd ed.; CRC Press: Boca Raton, FL, 1992.

(36) Chase, M. W., Jr.; Davies, C. A.; Downey, J. R., Jr.; Frurip, D. J.; McDonald, R. A.; Syverud, A. N. *JANAF Thermochemical Tables*, 3rd ed.; *J. Phys. Chem. Ref. Data*; American Chemical Society and the American Institute of Physics for the National Bureau of Standards, 1985; Vol. 14, Suppl. 1.

(37) In *NIST Chemistry WebBook*, NIST Standard Reference database Number 69, February 2000 Release. Vibrational frequency data compiled by M. E. Jacox.

(38) Shimanouchi, T., Tables of Molecular Vibrational Frequencies Consolidated Volume I, National Bureau of Standards, 1972; pp 1−160.

(39) Levine, Ira N. In *Molecular Spectroscopy*; Wiley: New York, 1975.

(40) *Thermodynamic Properties of Individual Substances*; Gurvich, L. V., Veyts, I. V., Alock, C. B., Eds.; Hemisphere: New York, 1992; Vol. 2.

(41) Chase, M. W., Jr. *J. Phys. Chem. Ref. Data* **1998**, Monograph 9, 1.

(42) Seetula, J. A. *J. Chem. Soc., Faraday Trans*. **1996**, *92*, 3069.

(43) Hudgens, J. W.; Johnson, R. D. I.; Timonen, R. S.; Seetula, J. A.; Gutman, D. *J. Phys. Chem*. **1991**, *95*, 4400.